Effect of the preequilibrium process upon fast neutron fission spectra from ^{238}U

T. Kawano
Department of Advanced Energy Engineering Science, Kyushu University, 6-1, Kasuga-kouen, Kasuga 816-8580, Japan

T. Ohsawa
Department of Nuclear Engineering, Kinki University, Kowakae, Higashi-Osaka 577-8502, Japan

M. Baba
Cyclotron and Radioisotope Center, Tohoku University, Aoba-ku, Sendai 980-8578, Japan

T. Nakagawa
Japan Atomic Energy Research Institute, Tokai-mura, Ibaraki-ken 319-1195, Japan
(Received 4 September 2000; published 26 January 2001)

A preequilibrium process for the prefission neutron which is emitted before scission is calculated with the model of Feshbach, Kerman, and Koonin. A forward-peaked angular distribution of the neutron emission from ^{238}U bombarded by 14 and 18 MeV neutrons is expressed with the statistical multistep compound process and the one-step direct process. The fission neutron energy spectra are calculated with the model of Madland and Nix, with some modifications by Ohsawa *et al.* The calculated total neutron emission spectra and their energy-angle distributions (double-differential cross sections) are compared with the experimental data, and a strength of the residual interaction V_0 is estimated. The comparisons of the calculations with the experimental data show that the 14 MeV data are well reproduced but the 18 MeV data are underestimated. Anisotropy is seen in the angle-differential fission spectra, and this is due to an existence of the prefission neutron.

DOI: 10.1103/PhysRevC.63.034601 PACS number(s): 24.10.−i, 24.60.Dr, 24.60.Gv, 25.85.Ec

I. INTRODUCTION

Recent progress in the quantum-mechanical approach to the preequilibrium nuclear reaction has brought about a good understanding of the smooth forward-peaked angular distributions which are observed in the particle emission spectra at high energy nuclear reactions. There are three well-known statistical multistep direct (MSD) theories; those are the theories of Feshbach, Kerman, and Koonin [1] (FKK), Tamura, Udagawa, and Lenske [2] (TUL), and Nishioka, Weidenmüller, and Yoshida [3] (NWY). Those theories employed different statistical assumptions for the multistep reactions; however, descriptions of the first step (one-step) are the same in principle [4]. A validation of the statistical assumption employed in the various theories is still under discussion [5], but the difference among those theories may appear in reactions at high incident energies. Therefore at low energies ($E_{in} \leqslant 20$ MeV), the one-step process as well as the multistep compound (MSC) process can be adopted to analyze an experimental particle emission spectrum.

In Ref. [6] we showed that double-differential cross sections at incident energies below 20 MeV were reproduced by the incoherent sum of one-step MSD and MSC calculations, where a MSC correction factor was introduced. Up to now such analyses have been carried out by many authors, but those efforts concentrated on analyses of an inelastic scattering process or a charge exchange reaction, and so far no analysis with quantum-mechanical theories has done for a fission neutron spectrum.

The fission neutron spectra from ^{238}U bombarded by high energy neutrons show a forward-peaked angular distribution [7,8], and one can recognize that this anisotropy is due to a prefission neutron which is emitted before scission. The mechanism of the prefission neutron is the same as the preequilibrium nuclear reaction, and it is able to study this process in the MSC and MSD frameworks. Such an approach was examined for ^{239}Pu reactions by Chadwick and Young [9], but an investigation of the angular distributions has not been done.

On the other hand, a prompt neutron fission spectrum has often been represented by simple functions such as a Maxwellian-type or a Watt-type formula. Madland and Nix [10,11] proposed a new theory to express the prompt neutron fission spectra, and their theory reproduced the experimental fission spectrum data fairly well. Following the work of Madland and Nix, Ohsawa and co-workers [12–16] improved it to give a better fit of the experimental data. However, the prefission neutron emission in a multiple-chance fission process was represented by simple evaporation from a highly excited compound nucleus; then, neutron emission results in being isotropic. At higher energies, the prefission neutron removes a large momentum from the composite nucleus, and it may affect the multiple-chance fission process considerably.

Boikov *et al.* [17,18] analyzed the neutron emission spectra from 14.7 MeV neutron induced fission reactions of Th, U, and Np isotopes, and they included the preequilibrium effect in the prefission neutron. However, they applied an exciton model, so that the angular distributions of the emitted neutron were not calculated. If one investigates the quantum-mechanical effect in the fission neutron spectrum, the emitted neutrons may have a forward-peaked nature, and this is consistent with the experimental findings.

II. ANALYSIS

A. FKK model to the prefission neutron

When a high energy neutron collides with a fissionable nucleus, the neutron can be emitted before the composite system reaches a fully equilibrium state, and the fission process occurs if an excitation energy of the residual nucleus is larger than the fission threshold. An energy spectrum and an angular distribution of the prefission neutron can be analyzed with the MSD-MSC model of FKK [1]. There is no interference between preequilibrium and fission processes because preequilibrium takes place on a fast time-scale compared to slow fission decay. Therefore no formal modifications are needed to the FKK model. The FKK model gives an inclusive cross section which can be written as $(n,n'X)$, so that the cross section includes processes other than fission.

We analyze here relatively the low energy experimental data of Baba *et al.* [7,8]. The prefission neutron can be represented by the MSC as well as the one-step MSD process. The MSC spectrum is assumed to be isotropic. The double-differential cross section from the MSC process is given by [1]

$$\left(\frac{d^2\sigma}{d\Omega dE}\right)^{\mathrm{MSC}}=\frac{1}{4\pi}\frac{\pi}{k^2}\sum_J (2J+1)2\pi\frac{\langle\Gamma_{1J}\rangle}{\langle D_{1J}\rangle}\times\sum_N\sum_{\nu j}\frac{\langle\Gamma_{NJ}^{\uparrow\nu j}\rho^\nu(U)\rangle}{\langle\Gamma_{NJ}\rangle}\prod_{M=1}^{N-1}\frac{\langle\Gamma_{MJ}^{\downarrow}\rangle}{\langle\Gamma_{MJ}\rangle}, \quad (1)$$

where N is the class of preequilibrium states, j is the angular momentum of the emitted particle, ν labels the three exit modes ($\Delta N=0$ and ± 1), $2\pi\langle\Gamma_{1J}\rangle/\langle D_{1J}\rangle$ is the entrance strength for producing bound two-particle–one-hole (2p-1h) states of spin J, $\langle\Gamma_{NJ}^{\uparrow\nu j}\rho^\nu(U)\rangle$ is the escape width, $\langle\Gamma_{MJ}^{\downarrow}\rangle$ is the damping width, and $\langle\Gamma_{NJ}\rangle$ is the total width. Those quantities are calculated quantum mechanically as in Refs. [6,19,20]. A constant wave-function approximation is used, and the MSC correction factor 1/2 is included [6] (note that the factor $3/2R$ in Ref. [6] is a mistake).

The one-step MSD cross section is calculated as a distorted-wave Born approximation (DWBA) cross section which excites a 1p-1h state in the continuum. In order to avoid ambiguities in the MSD calculation method [5,21], an explicit formulation is given here although it is redundant. The DWBA cross section is given by [22]

$$\left(\frac{d\sigma}{d\Omega}\right)_{1\ \mathrm{step}}=\frac{2I_B+1}{(2I_A+1)(2s_a+1)}\frac{\mu_a\mu_b}{(2\pi\hbar^2)^2}\frac{k_b}{k_a}\times\sum_{\lambda m m_b m_a}|T_{ls\lambda}^{m m_b m_a}(\theta)|^2, \quad (2)$$

where a is the incident particle (s_a, l_a, j_a, and m_a), b the outgoing particle (s_b, l_b, j_b, and m_b), A the target state (0p-0h), B the residual state (1p-1h), l the orbital angular momentum transfer, s the spin transfer, and λ the total spin transfer ($\boldsymbol{\lambda}=\boldsymbol{l}+\boldsymbol{s}=\boldsymbol{I}_B-\boldsymbol{I}_A=\boldsymbol{j}_a-\boldsymbol{j}_b$). The transition matrix element $T_{ls\lambda}^{m m_b m_a}(\theta)$ is given in Ref. [22] with an appropriate form factor $f_{ls\lambda}(r)$ which represents the p-h excitation.

We assume that the nucleon-nucleon interaction has the Yukawa form. For the sake of simplicity, the spin transfer is neglected; then, $l=\lambda$. The form factor $f_{\lambda 0\lambda}(r)$ can be calculated as [23]

$$f_{\lambda 0\lambda}(r)=\sqrt{4\pi}\sqrt{2}V_0\hat{I}_B^{-1}(-1)^{\lambda-j_h-1/2}i^{l_p-l_h+\lambda}\hat{j}_h\hat{j}_p\times\langle j_p j_h 1/2,-1/2|\lambda 0\rangle\int u_p(r')g_\lambda(r',r)u_h(r')dr', \quad (3)$$

$$g_\lambda(r',r)=\frac{1}{\alpha\sqrt{rr'}}K_{\lambda+1/2}(\alpha r_>)I_{\lambda+1/2}(\alpha r'_<), \quad (4)$$

where l_p, l_h, j_p, and j_h are the quantum numbers of the single-particle states, $I(r)$ and $K(r)$ the modified Bessel functions, α^{-1} the range parameter, and V_0 the strength of effective interaction. Parity conservation demands that $j_p+j_h+\lambda=\text{even}$.

Equation (2) represents an excitation of a certain p-h pair in the shell structure with an angular momentum transfer of λ. To calculate the continuum excitation, one has to calculate all p-h pairs which satisfy the energy, spin, and angular momentum conservations [21]. Instead of that, it is possible to obtain the one-step cross section by an averaging of a certain number of calculated cross sections in Eq. (2), and it is multiplied by a phenomenological state density [19].

It is often assumed that the target spin is zero, $I_A=0$, so $I_B=\lambda$; the cross section is given by

$$\left(\frac{d^2\sigma}{d\Omega dE}\right)^{\mathrm{MSD}}_{1\ \mathrm{step}}=\sum_\lambda\frac{2\lambda+1}{2s_a+1}\frac{\mu_a\mu_b}{(2\pi\hbar^2)^2}\frac{k_b}{k_a}\times\overline{\sum_{m m_b m_a}|T_\lambda^{m m_b m_a}(\theta)|^2}\,\omega(p,h,E_x)R_n(\lambda), \quad (5)$$

where $\omega(p,h,E_x)$ is the density for the p-particle h-hole state at the excitation energy of E_x, and $R_n(\lambda)$ the spin distribution for n excitons ($n=p+h$). We use the expression of Běták and Dobeš [24] for $\omega(p,h,E_x)$, and a Gaussian distribution is assumed for $R_n(\lambda)$ with the spin cutoff factor $\sigma^2=0.24nA^{2/3}$ [25]. The single-particle state density g in $\omega(p,h,E_x)$ is taken to be $g=A/13\ \mathrm{MeV}^{-1}$. The binding energies for the single-particle states are calculated with the Nilsson model parameters of Bengtsson and Ragnarsson [26].

B. Madland-Nix model to the fission neutron

The fission neutron spectra are calculated with the theory of Madland and Nix [10], modified by Ohsawa *et al.* [12–14]. The prompt neutron fission spectrum is calculated as a weighted average of spectra from both the light and heavy fragments,

$$\chi(E)=(\nu_L\chi_L(E)+\nu_H\chi_H(E))/(\nu_L+\nu_H), \tag{6}$$

where χ_L and χ_H are the normalized spectra from those fragments, and ν the average number of neutrons. The ratio of ν_L to ν_H is not well known at high energies, so $\nu_L=\nu_H$ is assumed.

The spectrum $\chi_{L,H}$ is given by [10]

$$\chi_{L,H}(E)=\frac{1}{2\sqrt{E_f}T_m^2}\int_{(\sqrt{E}-\sqrt{E_f})^2}^{(\sqrt{E}+\sqrt{E_f})^2}\sigma_R(\epsilon)\sqrt{\epsilon}d\epsilon \times\int_0^{T_m}k(T)T\exp^{-\epsilon/T}dT, \tag{7}$$

where E_f and T_m are the average energy and the maximum nuclear temperature of the fission fragments, $k(T)$ the temperature dependent normalization integral [10], and $\sigma_R(\epsilon)$ the inverse reaction cross section calculated with the optical model. The maximum temperature T_m can be related to the neutron binding energy B_n, the incident energy E_n, the total energy release E_r, and the total kinetic energy E_k as $aT_m^2=E_r+B_n+E_n-E_k$, where a is the level density parameter of the compound. The total energy release is calculated with the mass formula of Tachibana *et al.* [27], and the values of E_k are taken from measurements. The temperatures for the light and heavy fragments are determined from the relation $a_LT_{mL}^2+a_HT_{mH}^2=aT_m^2$. The level density formula of Ignatyuk *et al.* [28] is adopted for the fission fragments in order to include the shell effect.

Above the threshold energy of multiple-chance fission, (n,nf), $(n,2nf)$, etc., occur. The fission spectra for those reactions can be obtained by a weighted sum of the spectra from fission fragments and the spectra from a statistical decay before scission. The weight is calculated with the average number of neutrons, ν_i, and the fission probability P_{fi}, where i stands for the ith chance fission. When up to the second-chance fission processes contribute, the total spectrum is given by

$$\chi(E)=\frac{\nu_1\chi_1(E)P_{f1}+\{\psi_1(E)+\nu_2\chi_2(E)\}P_{f2}}{\nu_1P_{f1}+(1+\nu_2)P_{f2}}, \tag{8}$$

and the case for the third-chance fission is

$$\chi(E)=\frac{\nu_1\chi_1(E)P_{f1}+\{\psi_1(E)+\nu_2\chi_2(E)\}P_{f2}+\{\psi_1(E)+\psi_2(E)+\nu_3\chi_3(E)\}P_{f3}}{\nu_1P_{f1}+(1+\nu_2)P_{f2}+(2+\nu_3)P_{f3}}, \tag{9}$$

where $\psi_i(E)$ ($i=1$ and 2) are the prefission neutron spectra, and $\chi_i(E)$ is calculated by Eq. (7) but the excitation energy of the compound must be corrected by the neutron binding energies and the energies removed due to statistical decays. The average number of neutron ν_i is obtained from energy conservation, which is expressed as [11]

$$\nu=\frac{aT_m^2-E_\gamma}{\overline{S_n}+\overline{\epsilon}}, \tag{10}$$

where E_γ is total average prompt γ-ray energy, $\overline{S_n}$ the average fission fragment neutron separation energy, and $\overline{\epsilon}$ the average energy of the emitted neutrons.

III. RESULTS AND DISCUSSIONS

A. Double-differential cross section

Double-differential cross sections (DDX) of ^{238}U reactions at the neutron energies of 14.1 and 18 MeV were measured by Baba *et al.* [7,8]. To represent those DDX data we decompose them into various processes. Up to the third-chance fission processes are taken into account.

The first-, second-, and third-chance fission neutrons excluding the prefission neutrons are expressed by $\nu_1\sigma_{1f}\chi_1(E)$, $\nu_2\sigma_{nf}\chi_2(E)$, and $\nu_3\sigma_{2nf}\chi_3(E)$, where $\chi_i(E)$ is calculated by Eq. (7). The multiple-chance fission cross sections σ_{1f}, σ_{nf}, and σ_{2nf} can be obtained by a decomposition of the total fission cross section σ_f. Note that the first-chance fission cross section is denoted by σ_{1f} in order to distinguish from the total fission cross section σ_f.

The decomposed fission cross sections for ^{238}U are shown in Fig. 1. The total fission cross sections in this figure were obtained based on the least-squares fitting [29] to the experimental data. The decomposition of the total fission cross section was made by means of the method described in Ref.

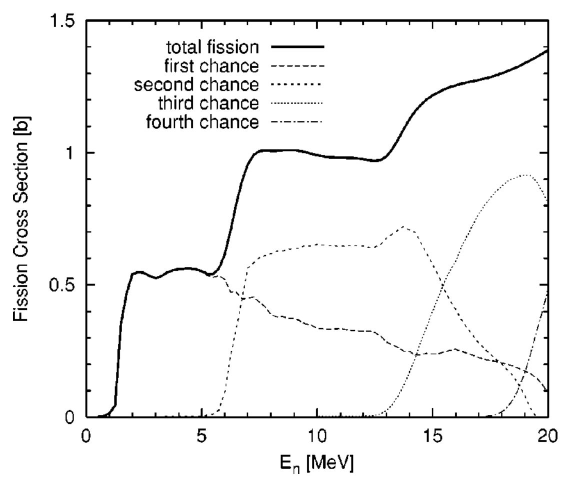

FIG. 1. Decomposition of the total fission cross sections of ^{238}U into the first-, second-, third-, and fourth-chance fission cross sections.

[10] using experimental data of the fission probability [30–33].

The inelastic scattering neutron $(n,n'X)$ has a normalized spectrum $\phi_1(E)$. Since it is an inclusive process, the cross section σ_{nX} is given by a sum of all possible neutron emission reactions; then, $\sigma_{nX}=\sigma_{n'}+\sigma_{2n}+\sigma_{3n}+\sigma_{nf}+\sigma_{2nf}$, and this is different from the first-chance prefission neutron spectrum $\psi_1(E)$ in Eqs. (8) and (9). The spectrum $\phi_1(E)$ has a forward-peaked angular distribution, and it is calculated with the MSC-MSD model as described previously.

For the $(n,2nX)$ and $(n,3nX)$ reactions, two or three neutrons are evaporated from the compound before scission. Those spectra are expressed as $\sigma_{2nX}\phi_2(E)$ and $\sigma_{3n}\phi_3(E)$, where $\sigma_{2nX}=\sigma_{2n}+\sigma_{3n}+\sigma_{2nf}$. The spectra $\phi_2(E)$ and $\phi_3(E)$ are assumed to be isotropic in the center-of-mass system, and those are calculated with the Hauser-Feshbach theory.

With the quantities defined above, the observable angle-integrated cross sections can be represented by

$$\frac{d\sigma}{dE}=\sigma_{nX}\phi_1(E)+\sigma_{2nX}\phi_2(E)+\sigma_{3n}\phi_3(E)+\nu_1\sigma_{1f}\chi_1(E)+\nu_2\sigma_{nf}\chi_2(E)+\nu_3\sigma_{2nf}\chi_3(E). \tag{11}$$

The double-differential cross section can be easily obtained by replacing $\phi(E)\rightarrow\phi(E,\theta)$, $\chi(E)\rightarrow\chi(E,\theta)$, etc. The cross sections for ^{238}U reactions have been well determined by experiments and theoretical calculations, so that we can utilize the evaluated cross sections [29,34].

B. Comparisons with the experimental data

An optical potential parameter of Madland and Young [35] is employed to calculate the reaction cross section and the transmission coefficients for the Hauser-Feshbach and MSC calculations. The same potential is used to generate distorted waves in the one-step MSD calculation. The Hauser-Feshbach calculations are carried out with the GNASH code [36]. The inverse reaction cross sections for fission fragments in Eq. (7) are calculated with the Walter-Guss global optical potential [37].

The adjustable parameter is the strength of effective interaction V_0 in Eq. (3). An absolute magnitude of the one-step MSD cross section is proportional to V_0^2; however, the total reaction cross section is conserved throughout the calculation, and an increase in the MSD process results in a decrease of a fraction of the statistical decay. Therefore V_0 determines the ratio of the preequilibrium to the compound emission.

The strength V_0 was searched for by fitting the calculated total neutron emission spectra to the experimental data at neutron incident energies of 14 and 18 MeV [7,8]. Values of 50.5 and 42.6 MeV were obtained for the 14 and 18 MeV data, respectively. Watanabe *et al.* [38] reported that V_0 is proportional to $E^{-1/2}$ although this relation was found for (p,p') reactions. Our results are roughly expressed by $V_0=185E^{-1/2}$. However, such a steep energy dependence has not been reported for (n,n') reactions. For fissionable nuclei

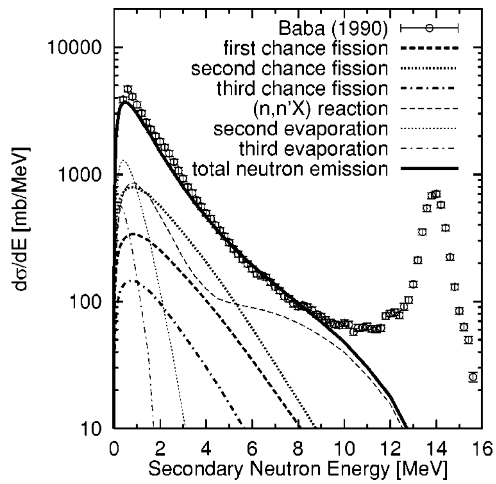

FIG. 2. Comparison of the calculated energy distribution of the emitted neutrons from ^{238}U at the incident neutron energy of 14 MeV with the experimental data. The thick dashed, dotted, and dot-dashed lines are the multiple-chance fission spectra but for the prefission neutrons. The spectra for the prefission neutrons including the contributions from inelastic, $(n,2n)$, and $(n,3n)$ reactions are shown by the thin lines.

the value of V_0 is not well determined because the preequilibrium emission has a small fraction to the total amount of neutron emission, and the number of fission neutrons is affected by uncertainties in the neutron multiplicities ν_i and fission probability P_{fi}. If one uses an averaged value $V_0=46.6\pm4$ MeV for both incident neutron energies, the calculations are still in good agreement with those data.

A comparison of the calculated angle-integrated neutron emission spectra with the experimental data [7] is shown in Fig. 2. The thick dashed, dotted, and dot-dashed lines are the fission spectra in which the prefission neutrons are excluded. The spectra for the prefission neutrons including the contributions from inelastic, $(n,2n)$, and $(n,3n)$ reactions are shown by thin lines, the dashed line is for the $(n,n'X)$ reaction, the dotted line is for $(n,2nX)$, and the dot-dashed line is for the $(n,3n)$ reactions. The calculation does not include elastic scattering and direct inelastic scattering to the collective levels in order to see the effect of preequilibrium clearly, so the calculated cross sections decrease monotonously above 8 MeV. Below 8 MeV the calculated spectrum agrees with the data well, and one can see clearly the contribution of the preequilibrium process above 5 MeV.

The double-differential cross sections were calculated at the scattering angles of 30°, 60°, 90°, 120°, and 150°. Comparisons of those with the experimental data are shown in Fig. 3. The one-step MSD components are only shown in those drawings, since the contributions from the other processes are isotropic. The preequilibrium effect can be observed at high energies, and the effect is more evident at forward angles. On the other hand, it is weak at backward angles and lower emission energies where fission spectra dominate. This feature of the preequilibrium process is well reproduced by inclusion of the FKK model in the fission spectrum calculations.

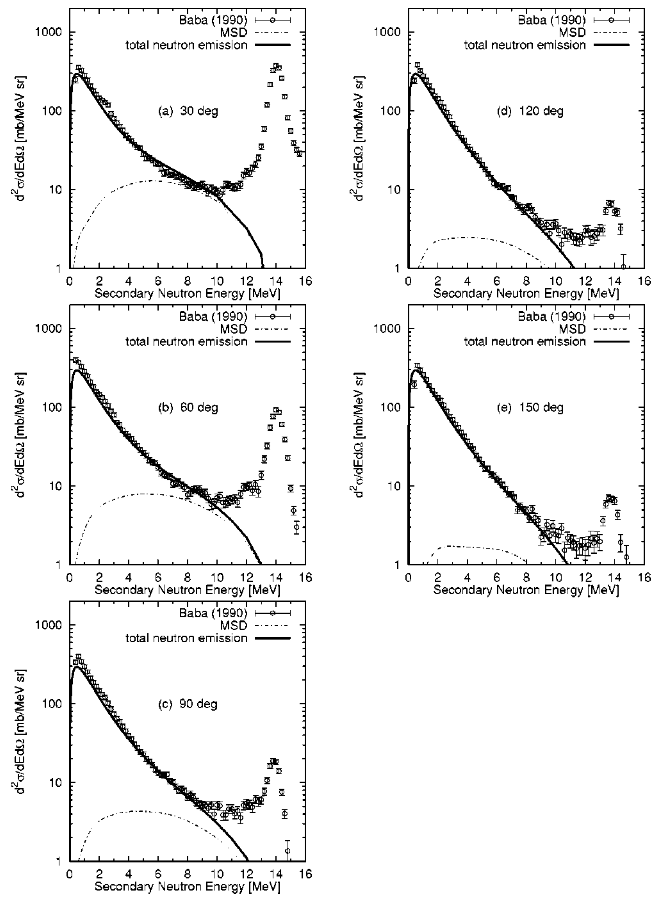

FIG. 3. Comparison of the calculated double-differential cross sections for ^{238}U at $E_n = 14$ MeV with the experimental data. The dot-dashed lines are the one-step MSD component, and the solid lines are the total emission spectra.

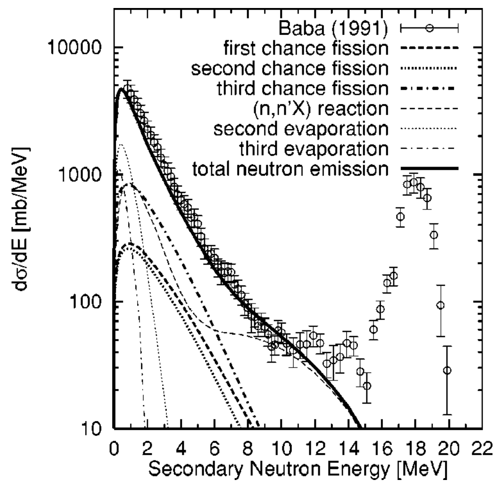

FIG. 4. Comparison of the calculated energy distribution of the emitted neutrons from ^{238}U at the incident neutron energy of 18 MeV with the experimental data. The thick dashed, dotted, and dot-dashed lines are the multiple-chance fission spectra but for the prefission neutrons. The spectra for the prefission neutrons including the contributions from inelastic, $(n,2n)$, and $(n,3n)$ reactions are shown by the thin lines.

Figure 4 shows a comparison of the calculated energy spectra at the incident energy of 18 MeV with the experimental data [8]. The elastic and the collective inelastic scattering cross sections are excluded in this study. As seen in the low energy region of this figure, the calculation is about 20% lower than the measurement. This disagreement is mainly due to the value of ν used. Since the fission spectra are multiplied by the ν values to give the total neutron emission, the uncertainty of ν directly influences the total magnitude of the emitted neutrons. The values of ν_i for each fission chances were estimated with the relation in Eq. (10), and the total ν value was renormalized to a reported value [39] since the total ν values have been determined by independent experiments and they have relatively small uncertainties ($\leqslant 2\%$). However, the decomposition of the total ν into each fission chance is still ambiguous.

The calculated double-differential cross sections are compared with experimental data in Fig. 5. One can see clearly the preequilibrium effect above 6 MeV, and these forward-peaked components are well reproduced with the one-step MSD contributions. The calculations underestimate the experimental data, which is also seen in the energy distribution in Fig. 4.

Recently the double-differential cross sections at 11.8 MeV were measured at the same institute [40]. It is interesting to compare our calculations with these data in order to see the validity of our calculation method. The same model parameters were used to calculate the fission spectra. Though the neutron energy of the experiment was 11.8 MeV, calculations were carried out at 12 MeV. The strength V_0 was calculated by the relation obtained in the 14 and 18 MeV data analyses, and it was 53.4 MeV.

The calculated double-differential cross sections are compared with the experimental data [40] in Fig 6. At scattering angles of 30° and 90°, the measured values were available above 6 MeV, but the whole spectra were measured at 60° and 120°. In the energy region 6–10 MeV one can see the preequilibrium emission clearly, and the magnitude of the calculated MSD process is in good accordance with the experimental data. Therefore it supports the relation $V_0 \propto E^{-1/2}$, as suggested by Watanabe *et al.* for proton-induced reactions [38]. At scattering angles of 60° and 120°, the calculated double-differential cross sections reproduced the experimental data well, from low energies up to 9 MeV.

C. Normalized fission neutron spectrum

A prompt neutron fission spectrum is often expressed by a normalized energy distribution as

$$\int_0^\infty \chi(E)dE = 1, \tag{12}$$

or more generally it can be expressed in the energy-angle differential form

$$\int_0^\pi \int_0^\infty \chi(E,\theta)\sin(\theta)dE\,d\theta = 1, \tag{13}$$

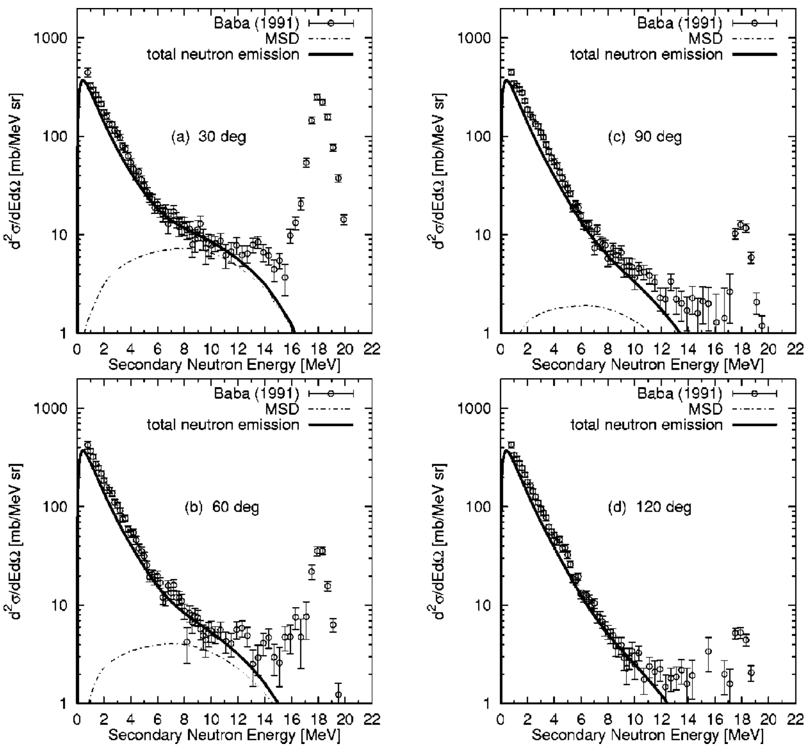

FIG. 5. Comparison of the calculated double-differential cross sections for ^{238}U at $E_n = 18$ MeV with the experimental data. The dot-dashed lines are the one-step MSD component, and the solid lines are the total emission spectra.

so that the spectra obtained are converted into this expression. The total spectra in Figs. 2 and 4 contain contributions of the reactions in which fission does not take place, such as (n,n') and $(n,2n)$; therefore, those processes should be excluded. We subtracted a contribution of the (n,n') reaction in which the excitation energy of the residual nucleus is lower than the fission barrier energy. On the other hand, we did not pay attention to the spectra from $(n,2n)$ and $(n,3n)$, because those contributions were small.

Normalized fission spectra at neutron-induced energies of 14 and 18 MeV are shown in Figs. 7 and 8, respectively. In Fig. 7, a small preequilibrium effect can be observed in the secondary neutron energy region 4–8 MeV. Above 8 MeV the fission neutron spectrum does not contain the prefission component, so that the preequilibrium effect is sharply cut off there, and its component is observed as inelastically scattered neutrons. Consequently the shape of the fission spectrum involves a bump near 7 MeV, which was reported by

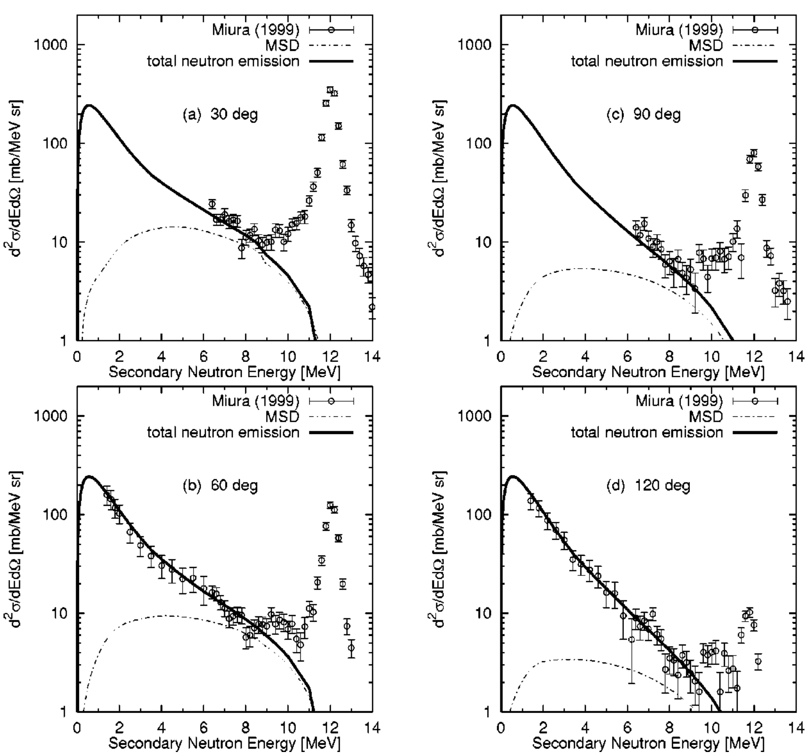

FIG. 6. Comparison of the calculated double-differential cross sections for ^{238}U at $E_n = 12$ MeV with the experimental data. The dot-dashed lines are the one-step MSD component, and the solid lines are the total emission spectra. The neutron incident energy of the experimental data is 11.8 MeV.

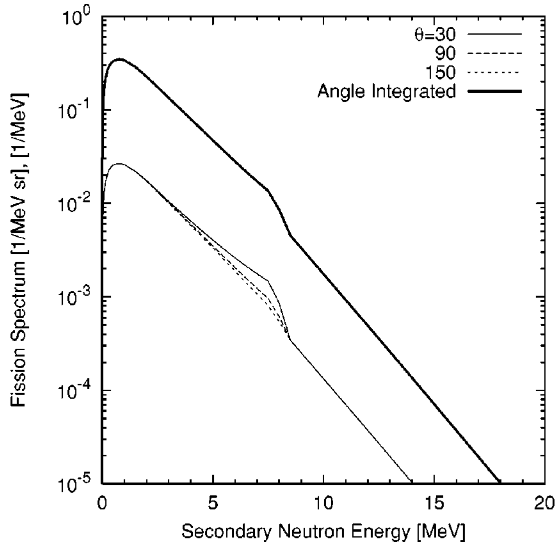

FIG. 7. Normalized prompt-neutron fission neutron spectra at the neutron incident energy of 14 MeV.

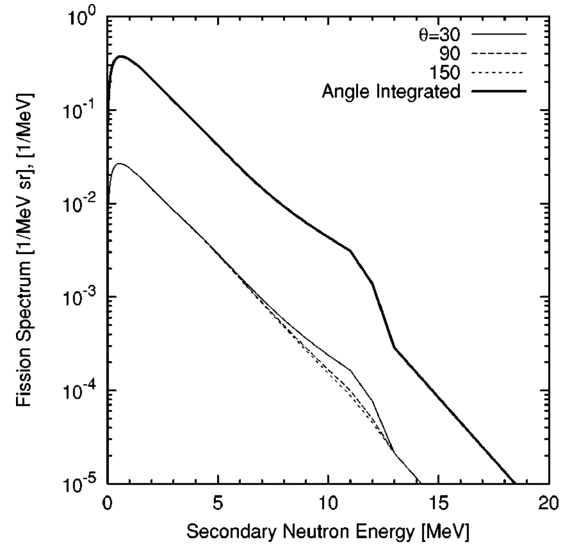

FIG. 8. Normalized prompt-neutron fission neutron spectra at the neutron incident energy of 18 MeV.

Boikov *et al.* [17]. Our analysis showed that this bump is larger at forward angles, but it can be ignored at backward angles.

In the case of the 18 MeV calculation in Fig. 8, one can see the effect of prefission neutron clearer than Fig. 7. A bump appears near 11 MeV, which is due to the sharp cutoff of the inelastic scattering component at the second-chance fission threshold, and the (n,n') reaction is connected smoothly above there to yield the total neutron spectrum as seen in Fig. 4. Because of the existence of the prefission neutron, the angle-differential spectra become anisotropic in the energy region 5–12 MeV.

IV. CONCLUSION

A fission neutron spectrum from the neutron-induced reactions on ^{238}U was decomposed into the preequilibrium, multiple-chance fission, and multiple neutron emission processes. The multiple-chance fission probabilities were obtained by experimental data. The Feshbach-Kerman-Koonin model was adopted for the preequilibrium neutron emission process to reproduce a forward-peaked angular distribution of the secondary neutrons. The fission neutron spectra for the multiple-chance fission process were calculated with the Madland-Nix model modified by Ohsawa *et al.*, and the FKK model calculation was incorporated into this model as a prefission neutron for the second-chance fission process.

Neutron emission spectra thus calculated were compared with the experimental data of double-differential cross sections at incident energies of 14 and 18 MeV. The strength of the effective interaction V_0 was determined for those measurements, and values of 50.5 and 42.6 MeV were obtained for the 14 and 18 MeV data, which were roughly expressed by $V_0 = 185E^{-1/2}$. The 14 MeV data were well reproduced by the present calculation method, not only the energy distribution but also angular distributions. However, the 18 MeV data were systematically underestimated. This underestimation is probably due to the average number of neutrons, ν_i, and the fission probabilities P_{fi} for each fission chance.

The calculations were carried out for 11.8 MeV double-differential cross section data, and it was found that our calculation method gave a good fit to the experimental data, and the relation $V_0 \propto E^{-1/2}$ still holds at this energy.

The fission spectra obtained were expressed in a normalized form. The preequilibrium effects in the fission spectrum appeared below the second-chance fission threshold. Because of the existence of the prefission neutron, the angle-differential spectra became anisotropic.

ACKNOWLEDGMENTS

We thank Dr. M.B. Chadwick for valuable discussions. One of the authors (T.K.) also acknowledges Dr. A. Marcinkowski for useful comments.

[1] H. Feshbach, A. Kerman, and S. Koonin, Ann. Phys. (N.Y.) **125**, 429 (1980).
[2] T. Tamura, T. Udagawa, and H. Lenske, Phys. Rev. C **26**, 379 (1982).
[3] H. Nishioka, H. A. Weidenmüller, and S. Yoshida, Ann. Phys. (N.Y.) **183**, 166 (1988).
[4] A. J. Koning and J. M. Akkermans, Ann. Phys. (N.Y.) **208**, 216 (1991).
[5] M. B. Chadwick, F. S. Dietrich, A. K. Kerman, A. J. Koning, S. M. Grimes, M. Kawai, W. G. Love, M. Herman, F. Petrovich, G. Walker, Y. Watanabe, H. Wolter, M. Avrigeanu, E. Betak, S. Chiba, J. P. Delaroche, E. Gadioli, S. Hilaire, M. S. Hussein, T. Kawano, R. Lindsay, A. Marcinkowski, B. Marianski, M. Mustafa, E. Ramström, G. Reffo, W. A. Richter, M.

A. Ross, and S. Yoshida, Acta Phys. Slov. **49**, 365 (1999).

[6] T. Kawano, Phys. Rev. C **59**, 865 (1999).

[7] M. Baba, H. Wakabayashi, N. Ito, K. Maeda, and N. Hirakawa, J. Nucl. Sci. Technol. **27**, 601 (1990).

[8] M. Baba, S. Matsuyama, T. Ito, N. Ito, K. Maeda, and N. Hirakawa, in *Proceedings of the International Conference on Nuclear Data for Science and Technology*, Jülich, Germany, 1991, edited by S. M. Qaim (Springer-Verlag, Berlin/Heidelberg, 1992), p. 349.

[9] M. B. Chadwick and P. G. Young, ''Calculated plutonium reactions for determining ^{239}Pu$(n,2n)^{238}$Pu,'' Los Alamos National Laboratory Report No. LAUR-99-2885, 1999 (unpublished).

[10] D. G. Madland and J. R. Nix, Nucl. Sci. Eng. **81**, 213 (1982).

[11] D. G. Madland, in *Proceedings of the International Conference on Nuclear Data for Science and Technology*, Gatlinburg, 1994, edited by J. K. Dickens (American Nuclear Society, LaGrange Park, IL, 1994), p. 532.

[12] T. Ohsawa and T. Shibata, in *Proceedings of the International Conference on Nuclear Data for Science and Technology* [8], p. 965.

[13] T. Ohsawa and T. Shibata, in *Proceedings of the International Conference on Nuclear Data for Science and Technology* [11], p. 639.

[14] T. Ohsawa, in *Proceedings of the 9th International Symposium on Reactor Dosimetry*, Prague, Czech Republic, 1996, edited by H. A. Abderrahim, P. D'hondt, and B. Osmera (World Scientific, Singapore, 1998), p. 656.

[15] T. Ohsawa, T. Horiguchi, and H. Hayashi, Nucl. Phys. **A653**, 17 (1999).

[16] T. Ohsawa, T. Horiguchi, and M. Mitsuhashi, Nucl. Phys. **A665**, 3 (2000).

[17] G. S. Boikov, V. D. Dmitriev, G. A. Kudyaev, Yu. B. Ostapenko, M. I. Svirin, and G. N. Smirenkin, Z. Phys. A **340**, 79 (1991).

[18] G. S. Boykov, V. D. Dmitriev, G. A. Kudyaev, V. M. Maslov, Yu. B. Ostapenko, M. I. Svirin, and G. N. Smirenkin, Ann. Nucl. Energy **21**, 585 (1994).

[19] M. B. Chadwick and P. G. Young, Phys. Rev. C **47**, 2255 (1993).

[20] R. Bonetti, M. B. Chadwick, P. E. Hodgson, B. V. Carlson, and M. S. Hussein, Phys. Rep. **202**, 171 (1991).

[21] A. J. Koning and M. B. Chadwick, Phys. Rev. C **56**, 970 (1997).

[22] G. R. Satchler, Nucl. Phys. **55**, 1 (1964).

[23] M. B. Johnson, L. W. Owen, and G. R. Satchler, Phys. Rev. **142**, 748 (1966).

[24] E. Běták and J. Dobeš, Z. Phys. A **279**, 319 (1976).

[25] H. Gruppelaar, ''IAEA advisory Group Meeting on Basic and Applied Problems on Nuclear Level Densities,'' Brookhaven National Laboratory Report, 1983 (unpublished), p. 143.

[26] T. Bengtsson and I. Ragnarsson, Nucl. Phys. **A436**, 14 (1985).

[27] T. Tachibana, M. Uno, M. Yamada, and S. Yamada, At. Data Nucl. Data Tables **39**, 251 (1988).

[28] A. V. Ignatyuk, K. K. Istekov, and G. N. Smirenkin, Yad. Fiz. **29**, 875 (1979) [Sov. J. Nucl. Phys. **29**, 450 (1979)].

[29] T. Kawano, H. Matsunobu, T. Murata, A. Zukeran, Y. Nakajima, M. Kawai, O. Iwamoto, K. Shibata, T. Nakagawa, T. Ohsawa, M. Baba, and T. Yoshida, J. Nucl. Sci. Technol. **37**, 327 (2000).

[30] J. D. Cramer and H. C. Britt, Phys. Rev. C **2**, 2350 (1970).

[31] B. B. Back, J. P. Bondorf, G. A. Otroschenko, J. Pedersen, and B. Rasmussen, Nucl. Phys. **A165**, 449 (1971).

[32] O. Hansen, B. B. Back, H. C. Britt, and J. D. Garrett, Phys. Rev. C **9**, 1924 (1974).

[33] G. N. Smirenkin and B. I. Fursov, ''The Dependence of the Fission Cross-sections for Heavy Nuclei on Neutron Energy in the ''Plateau'' Region,'' Report No. INDC(CCP)-292/L, 1989, p. 19.

[34] T. Nakagawa, K. Shibata, S. Chiba, T. Fukahori, Y. Nakajima, Y. Kikuchi, T. Kawano, Y. Kanda, T. Ohsawa, H. Matsunobu, M. Kawai, A. Zukeran, T. Watanabe, S. Igarasi, K. Kosako, and T. Asami, J. Nucl. Sci. Technol. **32**, 1259 (1995).

[35] D. G. Madland and P. G. Young, *Proceedings of the International Conference on Neutron Physics and Nuclear Data for Reactors and Other Applied Purposes*, Harwell, United Kingdom, 1978 (OECD, Paris, 1978), p. 349.

[36] P. G. Young and E. D. Arthur: ''GNASH, A Pre-equilibrium, Statistical Nuclear-Model Code for Calculation of Cross Sections and Emission Spectra,'' Report No. LA-6947, 1977.

[37] R. L. Walter and P. P. Guss, in *Proceedings of the International Conference on Nuclear Data for Basic and Applied Science*, Santa Fe, 1985, edited by P. G. Young, R. E. Brown, G. F. Auchampaugh, P. W. Lisowski, and L. Stewart (Gordon and Breach, New York, 1985), p. 1079; Radiat. Eff. **95**, 73 (1986).

[38] Y. Watanabe, A. Aoto, H. Kashimoto, S. Chiba, T. Fukahori, K. Hasegawa, M. Mizumoto, S. Meigo, M. Sugimoto, Y. Yamanouti, N. Koori, M. B. Chadwick, and P. E. Hodgson, Phys. Rev. C **51**, 1891 (1995).

[39] J. Frehaut, ''Coherent Evaluation of $\overline{\nu_p}$ for ^{235}U, ^{238}U, and ^{239}Pu,'' Report No. NEANDC(E) 238/L, 1986.

[40] T. Miura, M. Baba, M. Ibaraki, T. Win, T. Sanami, and Y. Hirasawa, ''Measurements of Double-Differential Neutron Emission Cross Sections of ^{238}U and ^{232}Th for 2.6, 3.6 and 11.8 MeV Neutrons,'' Ann. Nucl. Energy (to be published).